Biased Diffusion in a One-Dimensional Adsorbed Monolayer

O. Bénichou,[1] **A. M. Cazabat,**[2] **A. Lemarchand,**[1] **M. Moreau,**[1] **and G. Oshanin**[1]

We study the dynamics of a probe particle, which performs biased diffusive motion in a one-dimensional adsorbed monolayer composed of mobile hard-core particles undergoing continuous exchanges with a vapor phase. In terms of a mean-field-type approach, based on the decoupling of the third-order correlation functions into the product of pairwise correlations, we determine analytically the density profiles of the monolayer particles, as seen from the stationary moving probe, and calculate the terminal velocity V_{pr}, mobility μ_{pr} and the self-diffusion coefficient D_{pr} of the probe. Our analytical results are confirmed by Monte Carlo simulations.

1. INTRODUCTION

When a solid surface is brought in contact with an ambient gas phase, the interactions between the molecules of both systems often result in formation of a layer of gas particles covering the solid surface. Following a seminal work of Langmuir (see, e.g., in ref. 1), who has invented a somewhat simplified description in which the interactions between the adsorbed molecules were regarded as a mere hard-core, thermodynamic properties of such adsorbed layers, as well as different forms of possible phase transformations have been extensively studied and a number of important developments have been made. In particular, subsequent studies included more

---

[1] Laboratoire de Physique Théorique des Liquides (CNRS, UMR 7600), Université Pierre et Marie Curie, 75252 Paris Cedex 05, France.
[2] Laboratoire de Physique de la Matière Condensée, Collège de France, 75252 Paris Cedex 05, France.

realistic forms of intermolecular interactions or allowed for the possibility of multilayer formation. In consequence, more sophisticated forms of adsorption isotherms have been evaluated which explain quite well available experimental data (see, e.g., refs. 1–3).

Considerable effort has been also invested in understanding of molecular diffusion in adsorbed layers, which has a strong impact on their properties.[4, 5] Here, some approximate results have been obtained for both dynamics of an isolated adatom on a corrugated surface and collective diffusion, describing spreading of the macroscopic density fluctuations in interacting adsorbates being in contact with the vapor phase.[4–9] On the other hand, available studies of the tracer diffusion in adsorbed layers, which is observed experimentally in STM or field ion measurements and provides a useful information about such properties of monolayers as, e.g., their intrinsic viscosity, pertain to stricktly two-dimensional models excluding the possibility of particles adsoption or desorption (see, e.g., refs. 8–10 and references therein). Analysis of the tracer diffusion and mobility of impure molecules in adsorbed monolayers undergoing exchanges with the vapor phase seems to be lacking at present.

In this paper we study the time evolution of a model system consisting of a solid substrate covered by a monolayer of mobile hard-core particles undergoing continuous exchanges with a vapor, and a single impure, probe particle, which is subject to a constant external force E and hence performs a biased random walk constrained by hard-core interactions with the monolayer particles. Here, we concentrate on the one-dimensional case and model, in a usual fashion, the solid substrate as a regular one-dimensional lattice of adsorbing sites, which can support, at most, a single occupancy; results for the two-dimensional monolayer will be published elsewhere. In terms of a mean-field-type approach of ref. 11, which pressumes certain decoupling of the third-order correlation functions, we define the density profiles of the monolayer particles, as seen from the stationary moving probe, and determine analytically the probe terminal velocity $V_{pr}(E)$. In the most general case $V_{pr}(E)$ is obtained implicitly, as a solution of a non-linear equation relating its value to the system parameters. This equation simplifies in the limit of small E and here the probe velocity can be found explicitly; we show that it obeys $V_{pr}(E) \approx E/\zeta$, where the friction coefficient ζ, which is inverse of the probe mobility μ_{pr}, is expressed through the microscopic parameters characterizing the system under study. This result establishes the frictional drag force exerted on the probe by the monolayer particles in the low-E limit and thus can be thought off as the analog of the Stokes' law for the one-dimensional monolayer in contact with a vapor. Lastly, we determine the self-diffusion coefficient D_{pr} of the probe, which is computed here by assuming heuristically the validity of the Einstein relation

between the self-diffusion coefficient and the mobility. Our analytical results for the probe terminal velocity and the self-diffusion coefficient, as well as for the stationary density profiles around it are confirmed by Monte Carlo simulations of the corresponding master equation by the method of Gillespie.[15]

The paper is structured as follows: In Section 2 we formulate the model and introduce basic notations. In Section 3 we write down the dynamical equations which govern the time evolution of the monolayer particles and of the probe. Sections 4 and 5 are devoted to the analytical solutions of these evolution equations in the continuous-space limit and on the discrete lattice, respectively. In these sections we also present a comparison of the analytical results and Monte Carlo simulations data. Finally, we conclude in Section 6 with a brief summary and discussion of our results.

2. THE MODEL

The model consists of a one-dimensional regular, infinite in both directions lattice of spacing σ, the sites X of which are connected to a reservoir (a vapor phase) containing an infinite number of identical, electrically neutral gas particles (Fig. 1). The particles from the reservoir may adsorb onto the lattice sites, desorb from them or move along the lattice by performing symmetric random walk between the neighboring sites; adsorption onto the lattice and hops between the lattice sites are constrained by hard-core exclusion—each lattice site can be either singly occupied or vacant.
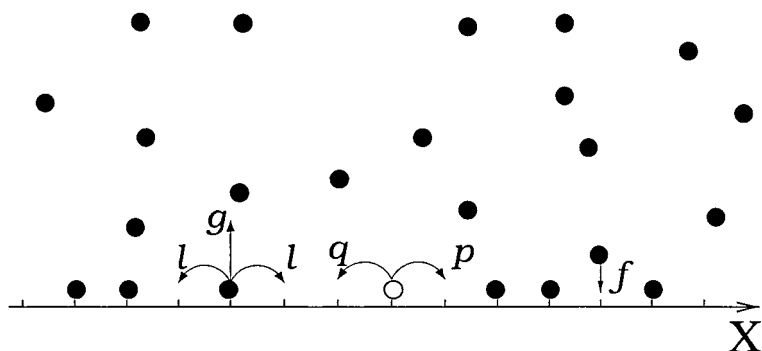

Fig. 1. One-dimensional lattice partially occupied by identical hard-core particles (filled circles) undergoing exchanges with the reservoir—the vapor phase. g, f, and l, $l = (1 - g)/2$, denote respectively particles desorption, adsorption and hopping probabilities. The open circle denotes the probe molecule, whose hopping probabilities are p and q, respectively.

The state of each lattice site X at time t is described by time-dependent occupation variable $\eta(X)$, which can take two values

$$\eta(X) = \begin{cases} 1, & \text{if the site } X \text{ is occupied by a gas particle} \\ 0, & \text{otherwise} \end{cases} \tag{1}$$

As one may readily notice, the just-described system corresponds to a one-dimensional version of the Langmuir adsorption/desorption model, with the only difference being that the lateral diffusion of the adsorbed molecules is allowed. Note, however, that the possibility of particles lateral diffusion makes the model more complicated, compared the Langmuir's one, since now the evolution of particle local densities at different sites is coupled due to diffusion.

Further on, we place at the site $X = 0$ at time $t = 0$ an extra particle, which will be referred to in what follows as the "probe," since it allows us to probe the resistance offered by the adsorbed layer to an external perturbance. Position of this particle at time t for a given realization of the process will be denoted as $X_{pr}(t)$. We stipulate that this particle is different from the monolayer particles in that it can not desorb back into the vapor phase, i.e., is constrained to move along the lattice only. Second, we suppose that this only particle is charged (for simplicity, we set the charge equal to unity in what follows) and is subject to a constant external electric field E, which favors its motion in a preferential direction. The questions which we address here are, first, the dependence of the probe particle terminal velocity $V_{pr}(E) = \lim_{t \to \infty} V_{pr}(t)$ on the magnitude of the driving force E and other system parameters; second, the form of the density profiles as seen from the stationary moving probe, and lastly, the self-diffusion coefficient of the probe in absence of the driving force.

Now, we define particle dynamics and system parameters more precisely:

(a) *Diffusion and Desorption.* Each of the adsorbed at time moment t gas particles waits a random, exponentially distributed time with mean τ^*, and then selects between either of three possibilities; it may choose to leave the lattice with a probability g, or attempt to hop, with the probability $l = (1 - g)/2$, to one of the two neighboring sites. If the desorption event is chosen—the particle leaves the lattice instantaneously. On the other hand, in case when the particle attempts to hop to one of the neighboring sites, the jump can actually occur only if the target site is empty; otherwise, the particle remains at its position.

(b) *Adsorption.* Particles of the reservoir wait a random, exponentially distributed time with mean[3] $\tau_{ad} = \tau^*$ and then attempt to adsorb onto the lattice with a probability f. As previously, an adsorption event takes place only if the chosen site is empty.

Note, that the total number of particles on the lattice is not conserved in such a dynamics. Mean density $\rho = \langle \eta(X) \rangle$, however, approaches as $t \to \infty$ a constant value

$$\rho_s = \frac{f}{f+g} \tag{2}$$

which relation is often called in the literature as the Langmuir adsorption isotherm.[1]

Here we suppose that parameters f and g are independent of each other and may take arbitrary values from the interval $[0; 1]$. In reality, their values are prescribed by the pressure of the gas phase, precise form of the solid-gas interaction potential and the temperature. As well, the latter determine the characteristic time τ^*, which is also considered here as an independent given parameter.

(c) *Dynamics of the Probe.* The probe particle waits an exponentially distributed time with mean τ, (which can be, in general case, different of τ^*) and then selects, at random, a jump direction: It chooses a right-hand or left-hand adjacent site with probabilities p and $q = 1 - p$, respectively. Similarly to the gas particles, the jump is only then fulfilled when the selected site is vacant at this moment of time.

In a usual fashion, the jump probabilities are related to the external electric field E, (oriented in the positive direction, such that $E \geqslant 0$), and the reciprocal temperature β by

$$p/q = \exp(\beta\sigma E) \tag{3}$$

where we have set the probe charge equal to unity. This relation together with the condition $p + q = 1$ defines the values of p and q.

3. EVOLUTION EQUATIONS

Let $P(X_{pr}, \eta; t)$ denote the probability of finding at time t the probe at the site X_{pr} and all other adsorbed particles in the configuration

---

[3] We choose for simplicity the same mean waiting time for the particles of the lattice and those in the reservoir; our results can be simply generalized for arbitrary τ_{ad} by replacement $f \to \tau^* f / \tau_{ad}$.

$\eta = \{\eta(X)\}$. Further on, let $\eta^{z,\,z+1}$ be the configuration obtained from η by exchanging the occupation variables of sites $X = z$ and $X = z+1$, i.e., $\eta(z) \leftrightarrow \eta(z+1)$, and η^z - the configuration obtained from η by replacement $\eta(X=z) \to 1 - \eta(X=z)$. Then, summing up all events which may change or result in a configuration (X_{pr}, η), we find that the time evolution of $P(X_{pr}, \eta; t)$ is guided by the following master equation:

$$
\begin{aligned}
\dot{P}(X_{pr}, \eta; t) = {} & \frac{1-g}{2\tau^*} \sum_{z \neq X_{pr}-\sigma,\, X_{pr}} \{ P(X_{pr}, \eta^{z,\,z+1}; t) - P(X_{pr}, \eta; t) \} \\
& + \frac{p}{\tau} \{ (1-\eta(X_{pr}))\, P(X_{pr}-\sigma, \eta; t) - (1-\eta(X_{pr}+\sigma))\, P(X_{pr}, \eta; t) \} \\
& + \frac{q}{\tau} \{ (1-\eta(X_{pr}))\, P(X_{pr}+\sigma, \eta; t) - (1-\eta(X_{pr}-\sigma))\, P(X_{pr}, \eta; t) \} \\
& + \frac{g}{\tau^*} \sum_{z \neq X_{pr}} \{ (1-\eta(z))\, P(X_{pr}, \eta^z; t) - \eta(z)\, P(X_{pr}, \eta; t) \} \\
& + \frac{f}{\tau^*} \sum_{z \neq X_{pr}} \{ \eta(z)\, P(X_{pr}, \eta^z; t) - (1-\eta(z))\, P(X_{pr}, \eta; t) \} \qquad (4)
\end{aligned}
$$

where the dot denotes the time derivative, the terms in the first three lines describe respectively the diffusion of the adsorbed gas particles and of the probe, which proceed due to the Kawasaki-type particle-vacancy exchanges, while the last two lines account respectively for the Glauber-type desorption and adsorption processes.

Equation (4) allows to compute the instantaneous velocity of the probe molecule. Multiplying both sides of Eq. (4) by X_{pr}, and summing over all possible states (X_{pr}, η) of the system, we find that:

$$
V_{pr}(t) = \frac{d\overline{X_{pr}(t)}}{dt} = \frac{\sigma}{\tau} \{ p(1-k(\sigma; t)) - q(1-k(-\sigma; t)) \} \qquad (5)
$$

where $\overline{X_{pr}(t)}$ denotes the mean displacement of the probe at time t and

$$
k(\lambda; t) = \sum_{(X_{pr}, \eta)} \eta(X_{pr}+\lambda)\, P(X_{pr}, \eta; t) \qquad (6)
$$

defines the probability of having at time t an adsorbed gas particle at distance λ from the probe, or in other words, can be interpreted as the monolayer density profile as seen from the moving probe.

Hence, in order to compute $V_{pr}(t)$ we have to determine the evolution of $k(\lambda; t)$. From Eq. (4) it follows that we have to consider separately the

evolution of $k(\lambda; t)$ for $|\lambda| > \sigma$ and $|\lambda| = \sigma$, since the monolayer particles dynamics is different in these two domains. We start first with the case $|\lambda| > \sigma$, in which domain the evolution of $k(\lambda; t)$ is not directly affected by the presence of the probe. In this case we find from Eq. (4) the following equation

$$\dot{k}(\lambda; t) = \frac{1-g}{2\tau^*} \{k(\lambda+\sigma; t) + k(\lambda-\sigma; t) - 2k(\lambda; t)\} - \frac{f+g}{\tau^*} k(\lambda; t) + \frac{f}{\tau^*}$$

$$+ \frac{p}{\tau} \sum_{(X_{pr}, \eta)} (1 - \eta(X_{pr}+\sigma)) \, P(X_{pr}, \eta; t)\{\eta(X_{pr}+\lambda+\sigma) - \eta(X_{pr}+\lambda)\}$$

$$- \frac{q}{\tau} \sum_{(X_{pr}, \eta)} (1 - \eta(X_{pr}-\sigma)) \, P(X_{pr}, \eta; t)\{\eta(X_{pr}+\lambda) - \eta(X_{pr}+\lambda-\sigma)\}$$
$$(7)$$

where the terms in the first line represent the contributions due to the particles diffusion, desorption and adsorption, while the terms in the last two lines are associated with the translation of the configuration $\eta \to \eta^{z, z \pm 1}$ due to the backward and forward hops of the probe particle. These terms are non-linear with respect to the occupation variables and thus couple the evolution of the "pairwise" correlation function $k(\lambda; t)$ to the evolution of the third-order correlations. Thus, to define the behavior of $k(\lambda; t)$ one faces the problem of solving an infinite hierarchy of coupled differential equations for the higher-order correlation functions.

Here we will resort to an approximate, mean-field-type decoupling scheme, which has been first applied in ref. 11 to describe tracer diffusion in a one-dimensional hard-core lattice gas with conserved number of particles, i.e., a gas for which the exchanges with the reservoir are forbidden and both f and g are equal to zero, while the ratio f/g is kept fixed. It has been shown in ref. 11 that results of such an approach are in a very good agreement with the Monte Carlo simulations data. Moreover, rigorous probabilistic analysis[13] of this model produced essentially the same results as ref. 11, thus proving that such a decoupling scheme renders exact description of the model. The reason why the decoupling is correct here is apparently due to the so-called propagation of local equilibrium; that is, in a large space-time scale, the system is locally in equilibrium, and the particle distribution is given by a set of product measures.[16] We note also parenthetically that a very good agreement between the numerical data and analytical predictions, based on the same decoupling scheme, have been observed for a slightly different model of hard-core gas spreading on a one-dimensional lattice from a reservoir connected to one of the lattice sites, in

which case density profiles do have a structure.[12] We thus adopt here this mean-field-type approach, which provides quite a good description of related dynamical models, and will verify in what follows our analytical predictions against the results of Monte Carlo simulations.

The decoupling scheme of ref. 11 is based on the assumption that the average with the weight $P(X_{pr}, \eta; t)$ of the product of several occupation variables of different sites factorizes into the product of their average values with the weight $P(X_{pr}, \eta; t)$. Namely, it assumes that the average product of the occupation variables factorizes as

$$\sum_{(X_{pr}, \eta)} \eta(X_{pr} + \lambda)(1 - \eta(X_{pr} \pm \sigma)) P(X_{pr}, \eta; t)$$

$$= \left\{ \sum_{(X_{pr}, \eta)} \eta(X_{pr} + \lambda) P(X_{pr}, \eta; t) \right\} \times \left\{ \sum_{(X_{pr}, \eta)} (1 - \eta(X_{pr} \pm \sigma)) P(X_{pr}, \eta; t) \right\}$$

$$= k(\lambda; t)(1 - k(\pm \sigma; t)) \tag{8}$$

Then, taking advantage of Eq. (8), we can rewrite Eq. (7), which holds for $|\lambda| > \sigma$, in the following form:

$$\dot{k}(\lambda; t) = \frac{1-g}{2\tau^*} \left\{ k(\lambda + \sigma; t) + k(\lambda - \sigma; t) - 2k(\lambda; t) \right\} - \frac{f+g}{\tau^*} k(\lambda; t)$$

$$+ \frac{f}{\tau^*} + \frac{p}{\tau} \left\{ 1 - k(\sigma; t) \right\} \left\{ k(\lambda + \sigma; t) - k(\lambda; t) \right\}$$

$$- \frac{q}{\tau} \left\{ 1 - k(-\sigma; t) \right\} \left\{ k(\lambda; t) - k(\lambda - \sigma; t) \right\} \tag{9}$$

Note, however, that despite the fact that the decoupling in Eq. (8) allows us to close the hierarchy in Eq. (7) at the level of pairwise correlations, the resulting equations still pose some technical problems for solving them; namely, they are non-linear with respect to $k(\lambda; t)$ differential equations. The method of solution will be discussed in the next two sections.

Now, similar analysis can be carried out to derive the dynamical equations, which govern the evolution of $k(\lambda; t)$ at points $|\lambda| = \sigma$. We find, respectively,

$$\dot{k}(\sigma; t) = \frac{1-g}{2\tau^*} \left\{ k(2\sigma; t) - k(\sigma; t) \right\} - \frac{f+g}{\tau^*} k(\sigma; t) + \frac{f}{\tau^*}$$

$$+ \frac{1}{\tau} \left\{ -qk(\sigma; t)(1 - k(-\sigma; t)) + p(1 - k(\sigma; t)) k(2\sigma; t) \right\} \tag{10}$$

and

$$\dot{k}(-\sigma; t) = \frac{1-g}{2\tau^*} \{k(-2\sigma; t) - k(-\sigma; t)\} - \frac{f+g}{\tau^*} k(-\sigma; t) + \frac{f}{\tau^*}$$
$$+ \frac{1}{\tau} \{-pk(-\sigma; t)(1 - k(\sigma; t)) + q(1 - k(-\sigma; t)) k(-2\sigma; t)\} \quad (11)$$

Equations (5) and (9)–(11) constitute a closed system of non-linear equations, which suffice the computation of the probe velocity and other characteristic properties.

4. STATIONARY SOLUTION OF THE EVOLUTION EQUATIONS IN THE CONTINUOUS-SPACE LIMIT.

Consider first the solution to Eqs. (5) and (9)–(11) in the continuous-space limit. Expanding $k(\lambda \pm \sigma; t)$ in Taylor series up to the second order in powers of σ (diffusion limit), we have that $k(\lambda; t)$ with $|\lambda| > 0$ obeys the following approximate equation:

$$\dot{k}(\lambda; t) = D_0 \frac{\partial^2 k(\lambda; t)}{\partial \lambda^2} + V_{pr}(t) \frac{\partial k(\lambda; t)}{\partial \lambda} - \frac{f+g}{\tau^*} k(\lambda; t) + \frac{f}{\tau^*} \quad (12)$$

where D_0 denotes the "bare" diffusion coefficient of the adsorbed gas particles, $D_0 = (1 - g) \sigma^2/2\tau^*$, and the velocity $V_{pr}(t)$ is now given by

$$V_{pr}(t) = \frac{p\sigma}{\tau} \{1 - k(\lambda = +0; t)\} - \frac{q\sigma}{\tau} \{1 - k(\lambda = -0; t)\} \quad (13)$$

Similarly, we find that Eqs. (9) and (10) take the form

$$\sigma\dot{k}(\lambda = +0; t)$$
$$= D_0 \frac{\partial k(\lambda; t)}{\partial \lambda}\bigg|_{\lambda = +0} + \left\{V_{pr}(t) - (f+g) \frac{\sigma}{\tau^*}\right\} k(\lambda = +0; t) + \frac{\sigma f}{\tau^*} \quad (14)$$

and

$$\sigma\dot{k}(\lambda = -0; t)$$
$$= -D_0 \frac{\partial k(\lambda; t)}{\partial \lambda}\bigg|_{\lambda = -0} - \left\{V_{pr}(t) + (f+g) \frac{\sigma}{\tau^*}\right\} k(\lambda = -0; t) + \frac{\sigma f}{\tau^*} \quad (15)$$

We turn next to the limit $t \to \infty$. Assuming first that the probe terminal velocity approaches some constant value $V_{pr}(E)$ as $t \to \infty$, i.e., $V_{pr}(E) = \lim_{t \to \infty} V_{pr}(t)$, we find the stationary solution $k(\lambda) = \lim_{t \to \infty} k(\lambda; t)$ of Eqs.(12), (14), and (15). This reads:

$$k(\lambda) = \rho_s [\, 1 + A_{\pm} \exp(-|\lambda|/\lambda_{\pm})\,] \tag{16}$$

In Eq. (16) ρ_s is determined by Eq. (2), the sign "$+$" ("$-$") corresponds to $\lambda > 0$ ($\lambda < 0$), the characteristic lengths $\lambda_{\pm}$ are given by

$$\lambda_{\pm} = \sigma \left\{ \sqrt{\left(\frac{V_{pr}(E)\,\sigma}{2D_0}\right)^2 + \frac{\sigma}{\sigma_{\text{eff}}}} \pm \frac{V_{pr}(E)\,\sigma}{2D_0} \right\}^{-1} \tag{17}$$

where the parameter σ_{eff} has the dimensionality of length, $\sigma_{\text{eff}} = D_0 \tau^*/\sigma(f+g)$, while the amplitudes $A_{\pm}$ in Eq. (16) obey

$$A_{\pm} = \pm \left(\frac{V_{pr}(E)\,\sigma_{\text{eff}}}{D_0}\right) \frac{1}{1 + \sigma_{\text{eff}}/\lambda_{\mp}} \tag{18}$$

Now several comments on the results in Eqs. (16)–(18) are in order. Note, first, that $\lambda_- > \lambda_+$, and consequently, the local density past the probe approaches its non-perturbed value ρ_s slower than in front of it; this signifies that correlations between the probe position and particle distribution are stronger past the probe and demonstrates the memory effects of the medium. Next, A_+ is always positive, while $A_- < 0$; this means that the density profile is a non-monotoneous function of λ and is characterized by a jammed region in front of the probe, in which the local density is higher than ρ_s, and a depleted region past the probe in which the local density is lower than ρ_s. It follows from Eqs. (16) to (18) that the depleted region dominates and the mean density in the adsorbed monolayer perturbed by the probe is lower than the mean density in the unperturbed monolayer; one finds from Eqs. (16) to (18) that the integral deviation Ω of the density from the equilibrium value ρ_s, i.e.,

$$\Omega = \int_{-\infty}^{\infty} \frac{d\lambda}{\sigma}\,(k(\lambda) - \rho_s) \tag{19}$$

is always negative,

$$\Omega = -\rho_s \left(\frac{V_{pr}(E)\,\sigma_{\text{eff}}}{D_0}\right)^2 \left[\, 1 + \frac{\sigma_{\text{eff}}}{\sigma} + \sqrt{\frac{4\sigma_{\text{eff}}}{\sigma} + \left(\frac{V_{pr}(E)\,\sigma_{\text{eff}}}{D_0}\right)^2}\,\right]^{-1} \tag{20}$$

which implies that the perturbance of the monolayer created by the driven probe shifts the balance between adsorption and desorption towards particles desorption into the reservoir. This result, however, is only an artefact of the continuous-space approximation. As we proceed to show in the next section, $\Omega \equiv 0$ and the mean density in the perturbed monolayer is still equal to ρ_s.

Now, we are in position to calculate the terminal velocity of the probe molecule. Substituting Eq. (16) into Eq. (13), we arrive at a closed-formed non-linear equation of the form

$$V_{pr}(E) = \frac{(p-q)(1-\rho_s)\,\sigma}{\tau} - \rho_s \sigma \; \frac{V_{pr}(E)\,\sigma_{\text{eff}}}{D_0 \tau} \left[\frac{p}{1+\sigma_{\text{eff}}/\lambda_-} + \frac{q}{1+\sigma_{\text{eff}}/\lambda_+} \right] \tag{21}$$

which determines $V_{pr}(E)$ implicitly. In Eq. (21) the first term on the rhs is a trivial, mean-field-type result, which obtains in the limit of, say, perfectly stirred monolayer with $D_0 \to \infty$ (or $\tau^* \to 0$). The second term on the rhs of Eq. (21), which is proportional to the Peclet-type number $P = V_{pr}\sigma_{\text{eff}}/D_0$ has a more complicated origin and is associated with collective effects— formation of a non-homogeneous, stationary density profile around the probe, whose characteristics depend themselves on the velocity.

Equation (21) is rather complicated and can be solved for arbitrary values of the system parameters only numerically. It simplifies considerably, however, in the limit $E \to 0$, in which case $V_{pr}(E)$ can be calculated analytically. Expanding p, q and $V_{pr}(E)$ in powers of E and retaining only linear in E terms, we find that in this limit $V_{pr}(E)$ attains the following, physically revealing form

$$V_{pr}(E) \approx \zeta^{-1} E \tag{22}$$

which can be thought off as the analog of the Stokes formula for driven motion in a one-dimensional monolayer undergoing continuous exchanges with the vapor phase. The friction coefficient in Eq. (22) is given explicitly by

$$\zeta = \frac{2\tau}{\beta\sigma^2(1-\rho_s)} \left[1 + \frac{\sigma\rho_s\sigma_{\text{eff}}}{D_0\tau(1+\sqrt{\sigma_{\text{eff}}/\sigma})} \right] \tag{23}$$

Note, that ζ is a sum of two contributions. The first one, ζ_{mf}, has an essentially mean-field-type form and is just a usual expression for the inverse mobility of a particle performing biased random walk on a one-dimensional lattice, divided by the fraction of non-occupied lattice sites, $(1-\rho_s)$,

which is the mean density of vacant sites in a monolayer with homogeneous particle distribution, i.e., monolayer being in equilibrium with the vapor phase. On contrary, the second term, ζ_{coop}, stems out of the cooperative effects, associated with formation of a stationary, non-homogeneous density profile around the probe, and represents the net resistance offered by the monolayer particles to the probe. It may be instructive to single out this contribution explicitly; setting $\tau = 0$, (which means physically that the probe slides on the surface without dissipation regardless of the surface corrugation), we have

$$\zeta_{\text{coop}} = \frac{2\tau^* \rho_s}{\beta \sigma^2 (1 - \rho_s)} \frac{1}{(f + g)(1 + \sqrt{D_0 \tau^* / \sigma^2 (f + g)})} \tag{24}$$

Comparing ζ_{mf} and ζ_{coop}, we infer that the latter becomes progressively more important in the limit, for instance, when both f and g tend to zero (while their ratio f/g is kept constant, $f/g = \text{const} = (1 - \rho_s)/\rho_s$). Of course, such a behavior can be expected on physical grounds since this limit corresponds to a lattice gas with a fixed number of particles and suppressed exchanges with the vapor phase; in this case the friction coefficient (as well as the characteristic lengths $\lambda_{\pm}$) is no longer constant, but rather diverges as $\zeta \sim \overline{X_{pr}(t)} \sim t^{1/2}$ in the limit $t \to \infty$.[11, 13]

Consider finally the situation with $E = 0$, in which case the terminal velocity vanishes and one expects conventional diffusive motion with the mean square displacement of the form

$$\overline{X_{pr}^2(t)} = 2D_{pr} t \tag{25}$$

where D_{pr} is some unknown function of the system parameters. Heuristically, we can compute D_{pr} for the system under study if we assume the validity of the Einstein relation $\mu_{pr} = \beta D_{pr}$ between the mobility μ_{pr}, $\mu_{pr} = \lim_{E \to 0} (V_{pr}(E)/E) = \zeta^{-1}$, and the self-diffusion coefficient D_{pr} of the probe particle (see for more details ref. 14). We find then that the probe self-diffusion coefficient should be given by

$$D_{pr} = \frac{\sigma^2 (1 - \rho_s)}{2\tau} \left[1 + \frac{\sigma \rho_s \sigma_{\text{eff}}}{D_0 \tau (1 + \sqrt{\sigma_{\text{eff}}/\sigma})} \right]^{-1} \tag{26}$$

In order to check our analytical predictions in Eqs. (16), (21), and (26), based on the approximate continuous-space Eq. (12), we have performed numerical Monte Carlo simulations of the system evolution using the method of Gillespie.[15] Results of these simulations, performed at different values of the parameters f, g, and p, are presented in Figs. 2 to 4.

These figures show that there is some systematic error between the analytical predictions of this Section, Eqs. (16), (21), and (26), and the numerical data; this error seems to be small when f is small but increases with increase of f or decrease of g, which means, apparently, that the error grows with the mean density of the monolayer. In particular, the maximal relative error R appears for $g = 0.3$ and amounts to 5.3, 7.7, and 7.9 per cent for Figs. 3, 4, and 5, respectively. Hence, the agreement is quite fair, and consequently, Eqs. (16), (21), and (26) can be regarded as rather accurate approximate results.

Now, one may attribute the origin of the discrepancy between the numerical and analytical results to the following two reasons. The first is,
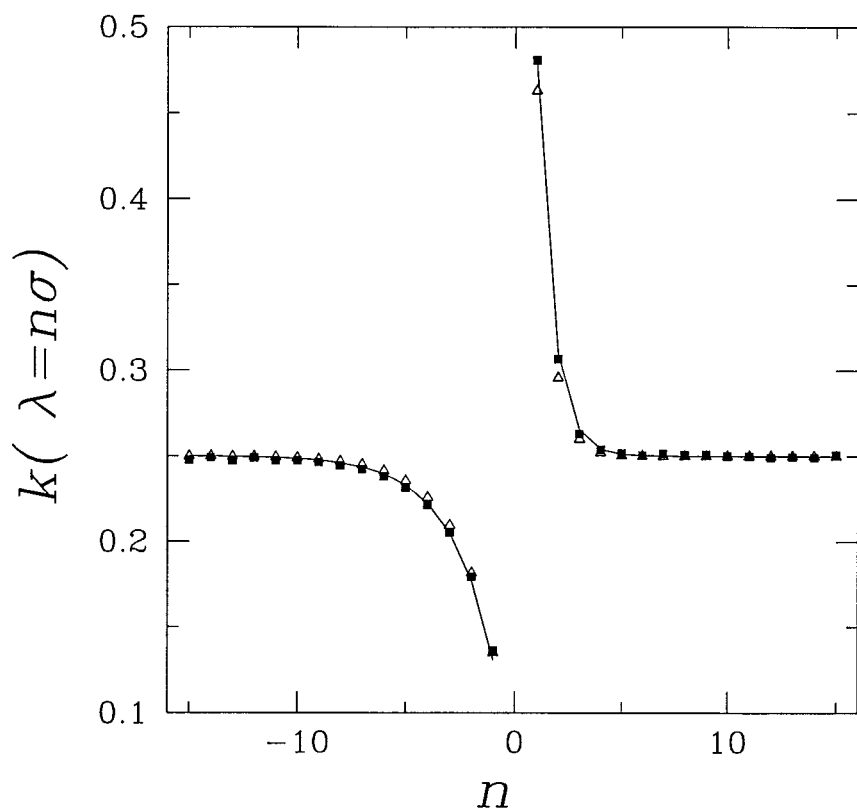

Fig. 2. Density profile around stationary moving probe molecule for $f = 0.1$, $g = 0.3$, and $p = 0.98$. The solid line is the plot of the solution, Eq. (32), of the discrete-space evolution equations. The empty triangles denote the corresponding solution in the continuous-space limit. Filled squares are the results of Monte-Carlo simulations.
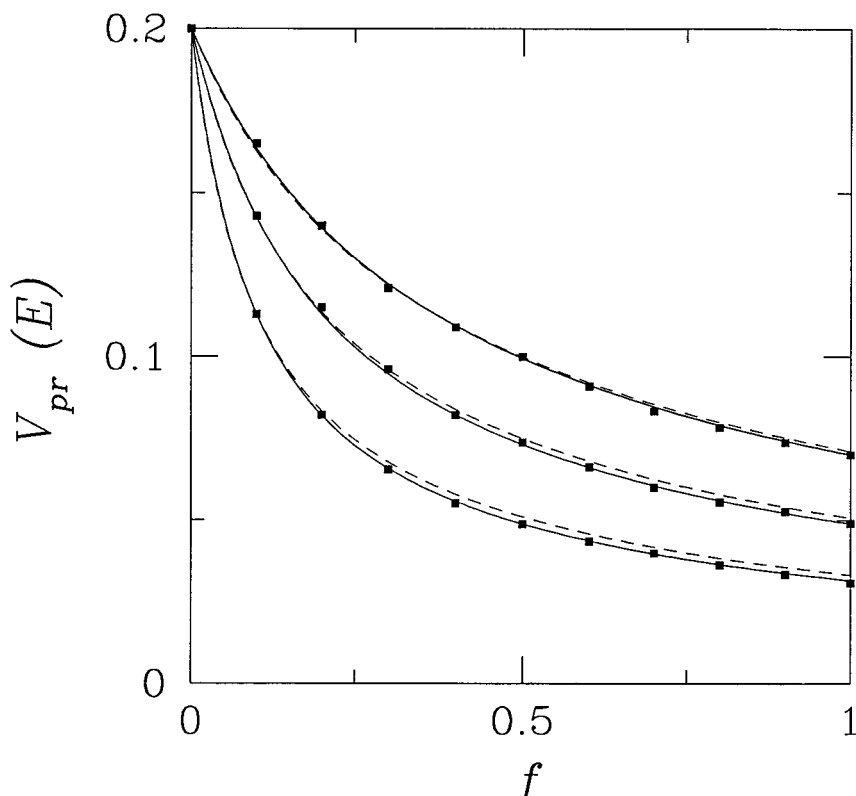
Fig. 3. Terminal velocity of the probe molecule as a function of the adsorption probability f at different values of the parameter g. The probe hopping probabilities are $p = 0.6$ and $q = 0.4$. The solid lines give the solution of Eqs. (36) and (37), the dashed lines—of Eq. (21), while the filled squares denote the results of Monte-Carlo simulations. Upper curves correspond to $g = 0.8$, the intermediate—to $g = 0.5$ and the lower—to $g = 0.3$, respectively.

evidently, the decoupling of the hierarchy of equations for the correlation functions in Eq. (8), which allowed us to close this hierarchy at the level of pairwise correlations. Despite the fact that such a decoupling scheme yields exact results for tracer diffusion in one-dimensional hard-core lattice gases with conserved number of particles,[11, 13] it may well be that it fails for systems in which the total number of particles is not conserved. Second, such a discrepancy may result from the fact that here solution of the discrete-space equations has been found by turning to a continuous-space limit; as a matter of fact, the only scaling limit in which Eq. (12) has some chance to be correct is speeding up the hopping of the particle by σ^2 and letting $\sigma \to 0$ (see ref. 17). We will show in the next section, that the latter
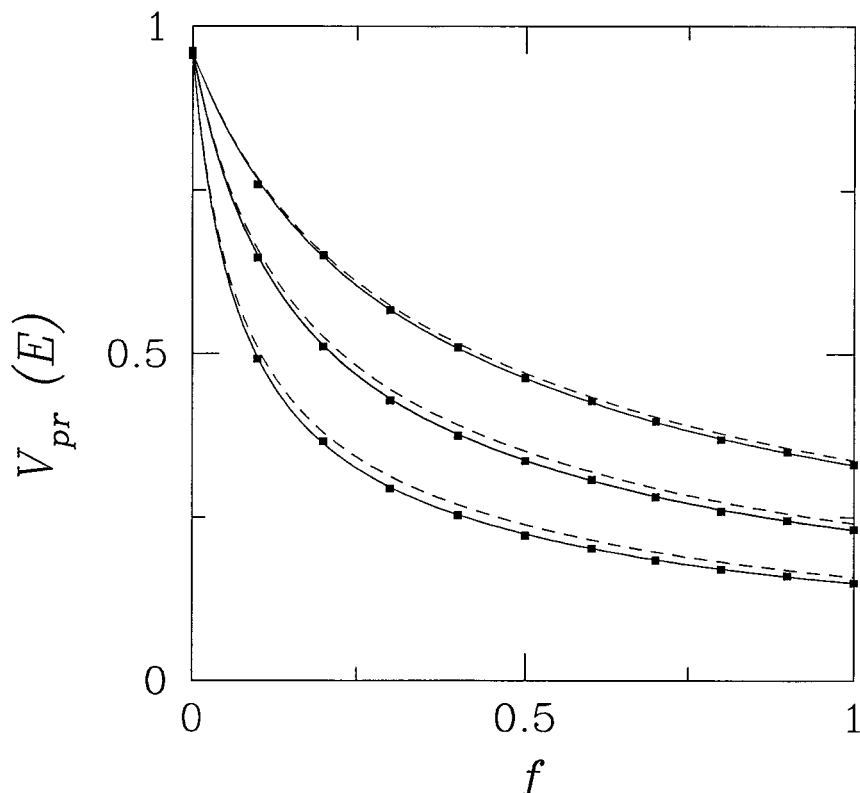
Fig. 4. Terminal velocity of the probe molecule as a function of the adsorption probability f. Notations and values of g are the same as in Fig. 3 except that the probe hopping probabilities are $p = 0.98$ and $q = 0.02$.

approximation is actually most crucial and the solution of the discrete-space equations (5), (9)–(11) is in a very good agreement with the numerical data. This implies, in turn, that the decoupling in Eq. (8) is also quite a plausible assumption for the system under study.

5. STATIONARY SOLUTION OF THE DISCRETE-SPACE EVOLUTION EQUATIONS.

Consider now the solution of the discrete-space (9)–(11) in the limit $t \to \infty$. Denoting $k_n = k(\lambda = n\sigma)$, and introducing auxiliary variables

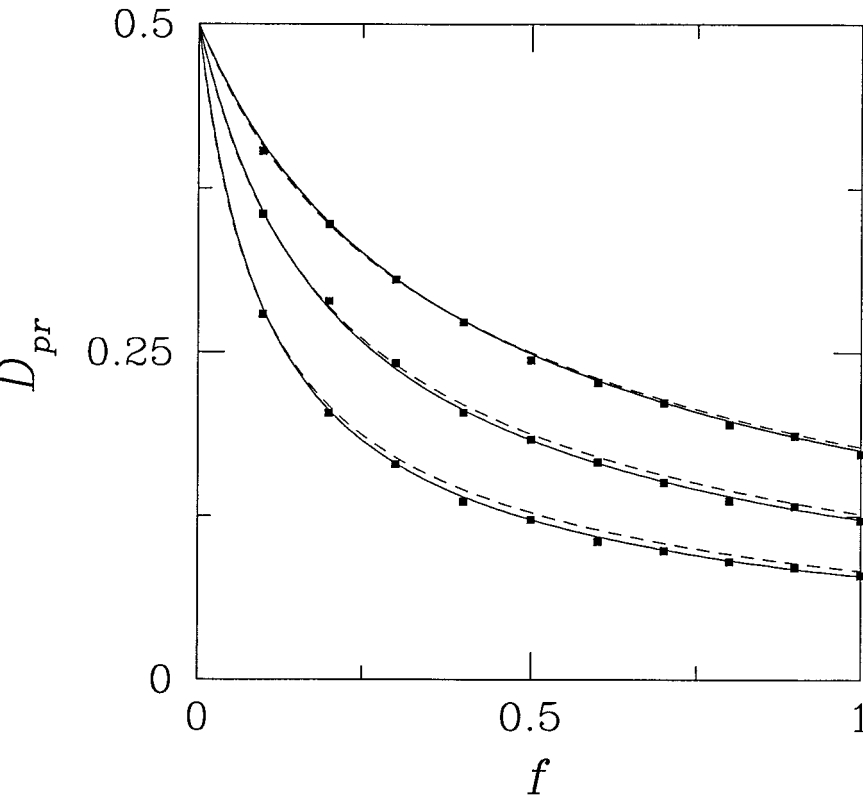$$z_1 = 1 + \frac{p\sigma^2}{D_0 \tau} (1 - k_1) \tag{27}$$

Fig. 5. Self-diffusion coefficient of the probe molecule as a function of the adsorption probability f. Notations and values of g are the same as in Figs. 3 and 4.

and

$$z_{-1} = 1 + \frac{q\sigma^2}{D_0\tau}(1 - k_{-1}) \tag{28}$$

in order to avoid too lengthy formulae, we can rewrite Eq. (9) in form of the following recursion relation

$$z_1 k_{n+1} - \left[z_1 + z_{-1} + \frac{\sigma}{\sigma_{\text{eff}}} \right] k_n + z_{-1} k_{n-1} + \rho_s \frac{\sigma}{\sigma_{\text{eff}}} = 0 \tag{29}$$

which holds for $|n| > 1$. Equation (29) has to be solved subject to the boundary conditions

$$z_1 k_2 - \left[z_{-1} + \frac{\sigma}{\sigma_{\text{eff}}} \right] k_1 + \rho_s \frac{\sigma}{\sigma_{\text{eff}}} = 0 \tag{30}$$

and

$$z_{-1} k_{-2} - \left[z_1 + \frac{\sigma}{\sigma_{\text{eff}}} \right] k_{-1} + \rho_s \frac{\sigma}{\sigma_{\text{eff}}} = 0 \tag{31}$$

Solution to these equations can be conveniently obtained by applying the discrete-space Fourier transformation, which yields an equation of essentially the same form as Eq. (16), i.e.,

$$k_n = \rho_s [1 + A'_\pm \exp(-\sigma |n|/\lambda'_\pm)] \tag{32}$$

with, however, different amplitudes $A'_\pm$ and different characteristic lengths $\lambda'_\pm$ compared to those given by Eqs. (18) and (17); we use here the prime to distinguish between the discrete and the continuous-space solutions. In the discrete-space Eq. (32) the characteristic lengths obey

$$\lambda'_\pm = \mp \sigma \ln^{-1} \left[\frac{z_1 + z_{-1} + (\sigma/\sigma_{\text{eff}}) \mp \sqrt{(z_1 + z_{-1} + (\sigma/\sigma_{\text{eff}}))^2 - 4 z_1 z_{-1}}}{2 z_1} \right] \tag{33}$$

while the amplitudes are given respectively by

$$A'_+ = \frac{z_1 - z_{-1}}{z_{-1} - z_1 \exp(-\sigma/\lambda'_+)} \tag{34}$$

and

$$A'_- = \frac{z_1 - z_{-1}}{z_{-1} \exp(-\sigma/\lambda'_-) - z_1} \tag{35}$$

Now, we are in position to obtain a system of equations, determining implicitly the unknown parameters z_1 and z_{-1}, which will allow us to compute the terminal velocity of the probe molecule; the latter is related to $z_{\pm 1}$ by $V'_{pr}(E) = D_0(z_1 - z_{-1})/\sigma$. Substituting Eq. (32) into Eqs. (27) and (28), we find

$$z_1 = 1 + \frac{p\sigma^2}{D_0 \tau} \left[1 - \rho_s - \rho_s \frac{z_1 - z_{-1}}{z_{-1} \exp(\sigma/\lambda'_+) - z_1} \right] \tag{36}$$

and

$$z_{-1} = 1 + \frac{q\sigma^2}{D_0\tau}\left[1 - \rho_s - \rho_s \frac{z_1 - z_{-1}}{z_{-1} - z_1 \exp(\sigma/\lambda'_-)}\right] \quad (37)$$

For arbitrary values of p, f, and g the parameters $z_{\pm 1}$, defined by Eqs. (36) and (37), and consequently, the terminal velocity $V'_{pr}(E)$ can be determined only numerically (see Figs. 3 and 4). However, $V'_{pr}(E)$ can be found analytically in the explicit form in the limit of a vanishingly small force E, $E \to 0$. Expanding $z_{\pm 1}$ in the Taylor series in powers of E and retaining only linear with E terms, i.e., setting

$$z_{\pm 1} \approx \alpha + \alpha\gamma_{\pm 1}E \quad (38)$$

where $\alpha = 1 + \sigma^2(1 - \rho_s)/2D_0\tau$, we find that coefficients $\gamma_{\pm 1}$ are determined by the system of two linear equations:

$$\alpha\gamma_1 = -\frac{\sigma^2\rho_s}{2D_0\tau}\frac{(\gamma_1 - \gamma_{-1})}{[\exp(\sigma/\lambda'_+(E=0)) - 1]} + \frac{\beta\sigma^3(1 - \rho_s)}{4D_0\tau} \quad (39)$$

and

$$\alpha\gamma_{-1} = -\frac{\sigma^2\rho_s}{2D_0\tau}\frac{(\gamma_1 - \gamma_{-1})}{[1 - \exp(\sigma/\lambda'_-(E=0))]} - \frac{\beta\sigma^3(1 - \rho_s)}{4D_0\tau} \quad (40)$$

which yield the Stokes-type law in Eq. (22) with the friction coefficient

$$\zeta' = \frac{2\tau}{\beta\sigma^2(1 - \rho_s)}\left[1 + \frac{\sigma\rho_s\sigma_{\text{eff}}}{D_0\tau}\frac{2}{1 + \sqrt{1 + 4\alpha\sigma_{\text{eff}}/\sigma}}\right] \quad (41)$$

Note, that similarly to Eq. (23) the friction coefficient ζ', calculated from the discrete-space evolution equations, is a sum of two terms; the first one describes a trivial, mean-field-type behavior and coincides with the result obtained within the continuous-space approximation. The second one, which is associated with the formation of a stationary, non-homogeneous density profile around the probe, is given explicitly by

$$\zeta'_{\text{coop}} = \frac{4\tau^*\rho_s}{\beta\sigma^2(1 - \rho_s)(f + g)}\frac{1}{1 + \sqrt{1 + 4\alpha\sigma_{\text{eff}}/\sigma}} \quad (42)$$

and has a different form compared to Eq. (24); Eq. (42) reduces to Eq. (24) only in the limit $\alpha\,\sigma_{\text{eff}}/\sigma \ll 1$.

Next, Eq. (41) allows to obtain the probe self-diffusion coefficient explicitly. Assuming again the validity of the Einstein relation, we find

$$D'_{pr} = \frac{\sigma^2(1-\rho_s)}{2\tau} \left[1 + \frac{\sigma\rho_s\sigma_{\text{eff}}}{D_0\tau} \frac{2}{1+\sqrt{1+4\alpha\sigma_{\text{eff}}/\sigma}} \right]^{-1} \qquad (43)$$

which has a different form compared to Eq. (26).

Lastly, we determine from Eqs. (32) to (35) an expression for the integral deviation from the equilibrium density. It follows then that Ω is given by

$$\Omega = A'_+ \frac{\exp(-\sigma/\lambda'_+)}{1-\exp(-\sigma/\lambda'_+)} + A'_- \frac{\exp(-\sigma/\lambda'_-)}{1-\exp(-\sigma/\lambda'_-)} \qquad (44)$$

Upon some lengthy calculations, we find that the rhs in Eq. (44) is exactly equal to zero. This implies that the perturbance created by the driven probe does not change the mean density of the adsorbed monolayer, contrary to the prediction in Eq. (20), based on the continuous-space approximation.

Comparison between the discrete-space solution and numerical data is presented in Figs. 2 to 5. We see now that Eqs. (36), (37), (32), and (43) agree with the Monte-Carlo results essentially better than their continuous-space counterparts; the maximal relative error is now independent of g and f, and amounts to only 1.9, 0.8, and 3 per cent for Figs. 3, 4, and 5, respectively. We note finally that despite this good agreement we certainly can not claim that Eqs. (36), (37), (32), and (43) provide an exact solution of the model.

6. CONCLUSIONS

To conclude, we have studied dynamics of a driven probe molecule in a one-dimensional adsorbed monolayer composed of mobile, hard-core particles undergoing continuous exchanges with the vapor phase. Within the framework of a decoupling procedure of ref. 11, based on the decomposition of the third-order correlation functions into a product of pairwise correlations, we have derived dynamical discrete-space equations describing evolution of the density profiles, as seen from the moving probe, and its velocity $V_{pr}(E)$. These equations have been solved both in the continuous-space (diffusion) limit, as well as in their original discrete-space form, which allowed us to check the appropriance of the continuous-space description. In both cases we have determined the probe particle terminal

velocity $V_{pr}(E)$ implicitly, as a solution of non-linear equations relating its value to the system parameters. We have shown that the discrete-space solution provides a very good agreement between analytical and numerical results, while the continuous-space approach can be regarded only as a rather accurate approximation. Further on, we have found that in the limit of a vanishingly small driving force the probe velocity attains the form $V_{pr}(E) \approx E/\zeta$, where E is the driving force and the friction coefficient ζ is expressed through the microscopic parameters characterizing the system under study. This result establishes the frictional drag force exerted on the probe by the monolayer particles in the low-E limit and thus can be thought off as the analog of the Stokes' law for the one-dimensional monolayer in contact with the vapor phase. Lastly, we have determined explicitly the self-diffusion coefficient D_{pr} of the probe, which result has been also confirmed by Monte Carlo simulations.

ACKNOWLEDGMENTS

REFERENCES

1. M.-C. Desjonquéres and D. Spanjaard, *Concepts in Surface Physics* (Springer-Verlag, Berlin, 1996).
2. T. L. Hill, *Statistical Mechanics* (Dover Publ., Inc., New York, 1987).
3. R. H. Fowler and E. A. Guggenheim, *Statistical Thermodynamics* (Cambridge University Press, London, 1939).
4. R. Gomer, *Rep. Prog. Phys.* **53**:917 (1990).
5. H. J. Kreuzer, in *Diffusion at Interfaces: Microscopic Concepts*, Springer Series in Surface Science, Vol. 12 (Springer-Verlag, Berlin, 1986).
6. M. A. Zaluska-Kotur and L. A. Turski, *Physica A* **195**:375 (1993).
7. Z. W. Gortel, M. A. Zaluska-Kotur, and L. A. Turski, *Phys. Rev. B* **52**:16916 (1995).
8. I. Vattulainen, J. Merikoski, T. Ala-Nissila, and S. C. Ying, in *Surface Diffusion: Atomistic and Collective Processes*, M. C. Tringides, ed. (Plenum Press, New York, 1997), and references therein.
9. K. W. Kehr and K. Binder, in *Application of the Monte Carlo Method in Statistical Physics*, K. Binder, ed. (Springer-Verlag, Berlin, 1987), and references therein.
10. J. De Coninck, G. Oshanin, and M. Moreau, *Europhys. Lett.* **38**:527 (1997).
11. S. F. Burlatsky, G. Oshanin, A. Mogutov, and M. Moreau, *Phys. Lett. A* **166**:230 (1992); S. F. Burlatsky, G. Oshanin, M. Moreau, and W. P. Reinhardt, *Phys. Rev. E* **54**:3165 (1996).
12. S. F. Burlatsky, G. Oshanin, A. M. Cazabat, M. Moreau, and W. P. Reinhardt, *Phys. Rev. E* **54**, 3832 (1996).

13. C. Landim, S. Olla, and S. B. Volchan, *Commun. Math. Phys.* **192**:287 (1998).

14. P. Ferrari, S. Goldstein, and J. L. Lebowitz, Diffusion, mobility and the Einstein relation, in *Statistical Physics and Dynamical Systems*, J. Fritz, A. Jaffe, and D. Szasz, eds. (Birkhäuser, Boston, 1985), p. 405.

15. D. T. Gillespie, *J. Comput. Phys.* **22**:403 (1976).

16. H.Spohn, *Large Scale Dynamics of Interacting Particles*, (Springer-Verlag, Berlin, 1991), Ch. 3

17. A. De Masi, P. A. Ferrari, and J. L. Lebowitz, *J. Stat. Phys.* **44**:589 (1986).